# Unveiling the stress-strain behavior of conjugated polymer thin films for stretchable device applications

Runqiao Song,<sup>1</sup> Harry Schrickx, <sup>1</sup> Nrup Balar, <sup>1</sup> Salma Siddika, <sup>2</sup> Nadeem Sheikh, <sup>1</sup> Brendan T. O'Connor<sup>1</sup>\*

Department of Mechanical and Aerospace Engineering, North Carolina State University, Raleigh, North Carolina 27695, United States

Department of Materials Science and Engineering, North Carolina State University, Raleigh, North Carolina 27695, United States

KEYWORDS: Polymer semiconductors, thin film mechanics, viscoelasticity, stretchable electronics, dynamic mechanical analyzer, Mullins' effect

ABSTRACT: The success of stretchable electronics based on conjugated polymers relies on having a thorough understanding of the polymer's mechanical behavior over conditions likely encountered during operation. To meet this need, a novel approach to capture the stress-strain response of thin conjugated polymer films is introduced. This is achieved by laminating the polymer film of interest on a thin elastomer substrate and testing the composite specimen in a dynamic mechanical analyzer in a tensile test configuration. We term this approach film laminated on thin elastomer (FLOTE) method. The benefits of this method include the ability to (1) determine the viscoelastic behavior of the conjugated polymer by testing over a broad range of temperatures and strain rates; (2) measure the film behavior over large cyclic strains including under in-plane compression; and (3) capture the impact of the neighboring elastomer on the behavior of the polymer film. The focus is on the widely studied poly(3-hexylthiophene) (P3HT) as a model system. We find that the viscoelastic characteristics of P3HT, varied by changing the specimen temperature, significantly impacts film stability under cyclic strain. This includes showing that the hysteresis behavior of the films under cyclic strain changes significantly with sample temperature. In addition, it is found that under cyclic loading the composite has features consistent with the Mullins' effect. Based on these results, insights into polymer viscoelastic characteristics necessary to achieve high-performance stretchable electronics are gained.

#### 1. Introduction

Stretchable electronics are poised to change how we interact with technology. The ability for electronics to change shape allows for new uses of existing technologies such as stowable displays,<sup>1</sup> as well as opens up new possibilities such as sensing in soft robotics.<sup>2,3</sup> Conjugated polymers are an attractive material system for stretchable electronics owing to excellent

electrical performance and favorable mechanical characteristics that can include large deformability. This has led to a number of demonstrations of stretchable devices employing conjugated polymers including solar cells, <sup>4-6</sup> transistors, <sup>7-10</sup> and LEDs. <sup>11</sup> In these demonstrations there have been a variety of design approaches that range from minimizing stresses in the active layers to intrinsically stretchable devices that employ polymers with suitable deformation characteristics. <sup>12</sup> Irrespective of the approach, the long term success is dependent on the mechanical response of the polymers employed being functional over the mechanical demands of the application. Thus, it is critical that the mechanical behavior of the conjugated polymers that are relevant to device operation is accurately captured, and that the key features enabling stable operation are resolved.

For intrinsically stretchable devices it is expected that the conjugated polymer will be placed under large tensile and compressive strains over a range of operating temperatures and strain rates. In most applications the devices will also be repeatedly stretched. Thus, there is a need to capture the stress-strain behavior of the polymer under these loading conditions. The conjugated polymers will also be integrated into multilayer devices and there is a need to understand the influence of neighboring layers on mechanical behavior. Most of the mechanical properties of interest can be captured in a tensile test. However, it is desirable to tests device relevant films which are typically under 200 nm thick, making them difficult to handle and incompatible with conventional tensile testers that lack the necessary sensitivity. As a result, a number of thin film mechanical testing methods have been developed.<sup>13-17</sup> A popular approach to measure the mechanical behavior of polymer thin films has been to probe the film while supported on a thick elastomer substrate, coined film on elastomer (FOE) tests.<sup>15,17,18</sup> Here, the elastic modulus mismatch between the film and substrate can result in a wrinkling instability when the thin film

is placed in compression, which allows one to calculate the Young's modulus of the film. 15,18,19 The FOE approach is also able to capture stress relaxation, ductility, and toughness. 17,20 However, due to the thick elastomer substrate employed, the method is unable to capture the full stress-strain response of the film.<sup>17</sup> Alternatively, tensile tests of pseudo free-standing films have been achieved by floating a polymer film on the surface of water.<sup>5,16,21,22</sup> In these film on water (FOW) tests, the full stress-strain characteristics of the film can be obtained. Yet, there are limitations with this approach that include the limited ability to vary the sample temperature due to the use of water. There is also the potential for the water to dissolve or swell the film of interest.<sup>22,23</sup> Just recently there has been a demonstration of tensile tests on completely freestanding polymer thin films.<sup>23</sup> However, handling a free-standing film under 200 nm thick can be quite challenging. The behavior of the film may also differ when adhered to a surface that should be understood for films that are integrated into multilayer devices. For example, the crack onset strain of a film can change significantly depending on the properties of a neighboring layer.<sup>24</sup> In addition, when considering the loading conditions likely encountered in an intrinsically stretchable device it is apparent that capturing in-plane compression behavior is desired. In both the FOW and free-standing film tensile tests there is an inability to place the film in compression. Thus, while a number of test methods have been introduced to probe film behavior, there remain a number of important characteristics for stretchable applications that are not captured.

To address the gaps in existing test methods we present a novel thin film measurement approach that we term Film Laminated on Thin Elastomer (FLOTE) method. In this approach, the polymer thin film of interest is laminated onto a thin elastomer support. The composite specimen is then loaded into a dynamic mechanical analyzer (DMA) to conduct a variety of

mechanical tests. By laminating the polymer film onto an elastomer support with thickness of 2 to 5 μm, the specimen can be handled relatively easily, while the elastomer is thin and soft enough that the stress-strain behavior of the film of interest is accurately captured. Importantly, the elastomer support provides a restoring force upon unloading, which can effectively put the thin film in compression. The restoring force also allows for cyclic strain tests. By using a composite structure, the impact of the neighboring elastomer layer on the polymer thin film can also be determined. Lastly, loading the specimen into a high-performance commercial DMA enables the tensile tests to be conducted over a large range of temperatures and strain rates. This large temperature range coupled with high-resolution stress and strain capabilities of the DMA allows for detailed viscoelastic characterization of the film. Capturing the viscoelasticity of the film is critical as it allows one to anticipate mechanical stability over broad operating conditions and gain a deeper understanding of the deformation mechanisms to better design stable stretchable devices.

Here we focus on the widely studied polymer semiconductor poly(3-hexylthiophene) (P3HT). The focus on P3HT is due to it being one of the most widely characterized polymer semiconductors, both electrically and mechanically.<sup>6,12,17,25-27</sup> This provides a material system that can be compared with other methods while also clearly showing how the FLOTE method provides advancements in film characterization. Below, we characterize the approach and use it to gain insight into P3HT deformation behavior. We demonstrate that the precise stress-strain response of the P3HT film can be extracted by applying an analytical parallel composite model. We also show that the restoring force of the strained elastomer results in the P3HT being placed in compression upon strain removal, enabling a view of compressive loading. We then characterize the stress-strain behavior of P3HT with changes in sample temperature and strain

rate. This includes demonstrating that the composite specimen can be used to effectively measure the stress relaxation of the polymer film over a broad time scale. The specimens are then tested over a large number of strain cycles revealing how the stress-strain characteristics evolve over numerous loading events. Through these measurements it is found that the viscoelastic state of the film plays a critical role in the film stress-strain response including hysteresis behavior under cyclic loading. In addition, we find the mechanical behavior of the composite specimen has characteristics consistent with the Mullins' effect. This includes softening after the first strain cycle and increased permanent set of the composite with increasing applied strains (i.e. elongation of the sample at zero stress upon strain removal). After presenting these findings we discuss the implications of the mechanical behavior on stretchable devices, including the expected impact of the observed strain softening, stress-strain hysteresis, and compressive stress on the thin film. As a result, the FLOTE method is found to be an effective approach to screen conjugated polymers for their potential implementation in stretchable device applications.

#### 2. Experimental methods

Polydimethylsiloxane (PDMS, Sylgard 184, Dow Corning) was chosen as the elastomer substrate, which was prepared by first dissolving the base and cross-linking agent in hexane with a concentration of 280 mg/ml. The solution was stirred for 30 minutes and then spun cast onto poly(4-styrenesulfonic acid) (PSS) coated glass substrates resulting in ~4 µm thick PDMS films. The PDMS base to crosslinking agent ratio was varied from 5:1 to 15:1 to modulate the stiffness of the elastomer substrate. PDMS was chosen as the supporting elastomer for several reasons including its large working temperature range. PDMS has a broad rubbery plateau with a glass transition below -125°C and a high temperature stability of over 200°C enabling measurements over a broad temperature range. P3HT was dissolved in chloroform or chlorobenzene at

5 to 20 mg/mL. The solution was spun cast at 1,000 rpm to 1,500 rpm on glass substrates coated with a PSS layer. The combination of solution concentration and spin cast speed resulted in film thickness to be between 20 nm to 250 nm. The P3HT film thickness was largely held at approximately 140 nm thick unless otherwise noted. The thickness of the thin PDMS and P3HT films was measured by variable angle spectroscopic ellipsometry and stylus profilometer.

To make the composite specimen, the PDMS film was first patterned into a dog bone shape by cutting with a blade. The dimensions of the dog bone were approximately 15 mm long and 5 mm wide in the narrow region of the specimen. The PDMS film was then transferred onto a thick PDMS slab (≈ 0.5 mm-thick) by laminating the PDMS film onto the thick PDMS and submerging the stack into water to dissolve the PSS layer between the thin PDMS and glass substrate. The P3HT film was also cut into the same dog-bone shape then transferred onto the PDMS thin film. This was done by laminating the P3HT film onto the PDMS stack and submerging into water to dissolve the PSS between the P3HT and glass substrate. The composite sample of P3HT and thin PDMS was then picked up from the thick PDMS slab and loaded into the DMA (TA instruments, DMA850) that is in a tensile test configuration. To pick up the specimen with minimal mechanical deformation, the thick PDMS was strained to make it stiff and was treated with octyltrychlorosilane (OTS) to minimize adhesion. The fabrication process is schematically presented in Figure 1(a). The specimen loaded into the DMA is shown in Figure **1(b)**. All DMA tests were conducted at a chamber temperature of 30°C unless otherwise stated. Tensile tests were also conducted on pseudo free-standing P3HT films and P3HT/PDMS composite samples using the FOW method. In this approach, the specimens are supported on water during the tensile test with details of the method described elsewhere.<sup>5</sup>

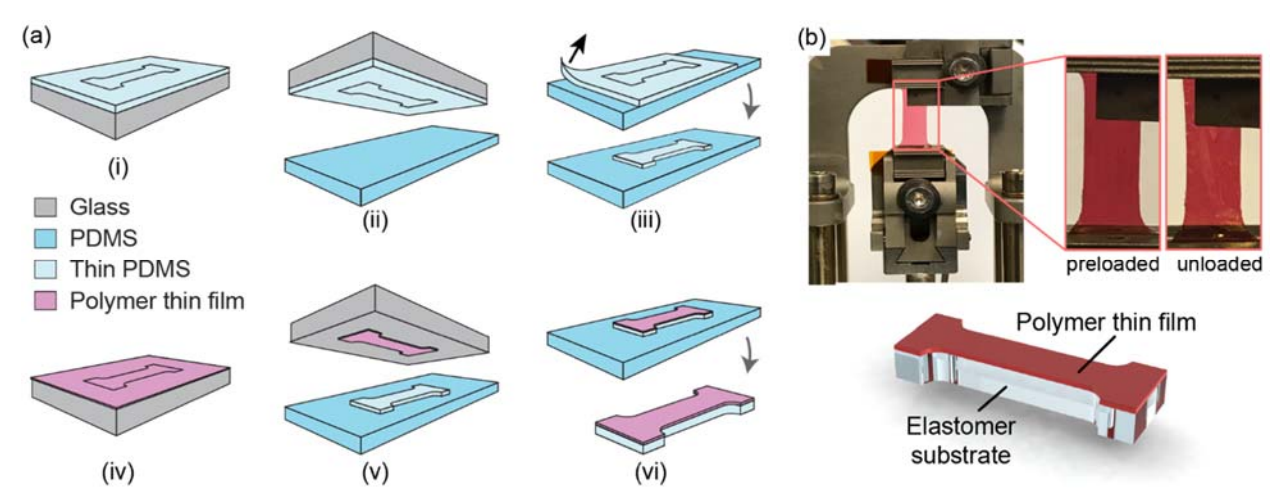


Figure 1. (a) A schematic of the processing steps to fabricate the dog-bone shaped FLOTE specimens that includes transferring the thin PDMS dog-bone to a thick PDMS substrate (i-iii) and transferring the polymer thin film onto the thin PDMS and removing the composite from the thick PDMS substrate (iv-vi). (b) Images of the FLOTE specimen loaded into the DMA before testing (preloaded) and after testing (unloaded) with an illustration of the specimen provided underneath.

#### 3. Results

#### 3.1. Method validation

Representative engineering stress-strain results of the P3HT/PDMS composite FLOTE specimen strained at a rate of 20%/min is given in **Figure 2(a)**. The specimen was strained to 30%, which is kept largely constant throughout this report for consistency. This strain is partly chosen as its well within the fracture limit of the P3HT films over the test conditions. During this test, the specimen is put under a small pre-load to ensure it is fully extended. However, given the soft and thin nature of the specimen, this can result in a small tensile strain of 0.5% - 1%. The amount of tensile strain initially on the specimen is estimated by determining the point of zero load upon strain removal after the first tensile load. The reported stress-strain curves include a linear extrapolation of the data from the small pre-strained condition to the no-load state. Along

with the composite specimen, the stress-strain behavior of the neat PDMS specimen is also given in **Figure 2(a)**. There is a clear difference in the force required to strain the composite relative to the neat PDMS specimen owing to the significantly stiffer P3HT relative to the PDMS. To extract the behavior of the P3HT, a parallel composite model was employed where the force (F) on the composite is be given by  $F_c = \sigma_c A_c = \sigma_s A_s + \sigma_f A_f$ , where  $\sigma$  is the stress, and A is the cross-sectional area. The subscripts c, s, and f, are for the composite, the substrate, and the polymer film respectively. The engineering stress in P3HT that is extracted from this model is plotted in **Figure 2(b)**.

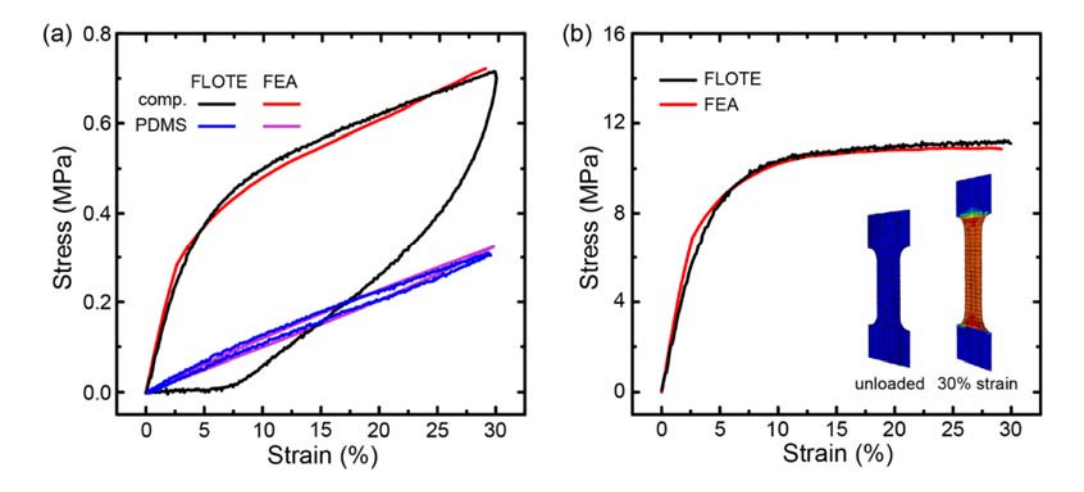


**Figure 2**. (a) The stress-strain characteristics of the FLOTE composite specimen and neat PDMS substrate. Also included are the finite element analysis (FEA) results for the composite and neat PDMS. The thickness of the P3HT was 140 nm and PDMS was 4 μm. (b) The stress-strain characteristics of the P3HT film from the FLOTE specimen extracted using a parallel composite model and the P3HT stress taken from the FEA. Inset, images of stress profile from the FEA model.

In the parallel composite model, no interface loads are considered across the polymer film and elastomer support (e.g. shear load) that may arise due to the different mechanical properties between the materials, such as Poisson's ratio. To determine if the parallel composite model is appropriate to capture the stress-strain response of the polymer thin film, we compare the results with finite element analysis (FEA) of the composite modeled in Abaqus. In the FEA model, the P3HT film was considered to be perfectly bonded to the PDMS substrate and the specimen geometry was set to match the experimental conditions. Additional details of the model are given in the supporting information. The mechanical behavior of the PDMS was first determined by fitting the experimental data to a hyperelastic model with Mullin's effect. The PDMS model matched the experimental data well as shown in Figure 2(a). The properties of the PDMS were then used in the FEA of the composite. To reproduce the experiment stress-strain response of the composite, the P3HT was assumed to be elastic-plastic by defining the Young's modulus, yield stress and strain hardening behavior after yield. The stress  $(\sigma_{11})$  – strain characteristics of the P3HT were then varied in the FEA model to fit the experimental tensile test results. The FEA modeled stress-strain behavior of the composite and the P3HT component are compared to the experimental data of the composite and the P3HT behavior extracted from the analytical composite model in Figure 2(a) and Figure 2(b), respectively. The stress profile of the strained sample from FEA is given in the inset of Figure 2(b). The results show good agreement between the FEA model and analytical composite model. The resulting shear stress on the P3HT ( $\sigma_{12}$  and  $\sigma_{32}$ ) calculated from the FEA model, assuming a Poisson's ratio of P3HT of 0.33 and PDMS of 0.49, were found to be several orders of magnitude lower than the in-plane normal stress ( $\sigma_{11}$ ), as shown in Figure S1. This demonstrates that the shear load on the P3HT is expected to be small and can be neglected.

While the FEA provides support that the analytical composite model accurately captures thin film behavior, a direct comparison to experimental data of a neat thin film is ideally needed. To approach this direct comparison, film on water tests were conducted for the composite specimen and pseudo-free standing P3HT films. Here, the specimen is floated on water to provide support that allows for sample manipulation and attachment to grips of a tensile tester.<sup>5,25</sup> The stressstrain behavior of the neat P3HT film is compared to the P3HT behavior extracted from the composite specimen in Figure S2. The two approaches result in similar stress-strain characteristics up to approximately 20% strain. The data begins to deviate where the neat P3HT film may begin to neck or fracture. The film on elastomer is expected to inhibit necking and extend the elongation at break. These results provide further support that the analytical composite model accurately captures the thin film behavior. Note that there were some minor differences in the stress-strain behavior of the FOW and FLOTE tests of the composite. We believe this is associated with differences in sample preparation and test conditions discussed further in the supporting information. Nevertheless, the simple parallel composite model is shown to accurately capture the neat P3HT behavior.

#### 3.2. Restoring force and film compression

One important aspect of the FLOTE method is the restoring force provided by the PDMS after extension. For large tensile strains, the polymer thin film deforms inelastically while the substrate deforms elastically. Upon the removal of the load the composite will first contract elastically. As the strain is reduced the tensile stress is removed from the polymer thin film while the elastomer remains in tension. The strain at which the force on the neat PDMS and the force on the composite are the same can be considered as the point where there is no load on the polymer thin film. Note that this assumes that no necking in the film takes place, which is

expected for well adhered films.<sup>30</sup> It also relies on the changes in cross-sectional area of the PDMS to be similar when tested alone or with P3HT attached, which is assumed to be the case. As the composite is further unloaded the elastomer continues to contract elastically and the polymer thin film is placed in compression. Thus, this approach is uniquely able to capture inplane compression of polymer thin films. As can be seen in Figure 2(a), the no-load strain for the thin film upon unloading the composite is 15.3%. As the strain in the composite is further reduced, the P3HT film is placed in compression. After the film is placed in compression, the elastic modulus mismatch between the film and substrate may result in film wrinkling, the film may also delaminate or yield, discussed further below.<sup>24</sup> At a certain point in the strain removal process, the tensile force on the PDMS and the compressive force on the film are equivalent and the total force is zero. Further strain reduction then leads to large out of plane buckling of the composite sample and a slightly negative stress that plateaus with continued strain removal. This permanent set of the composite is observed in Figure 2(a) at approximately 7.5% strain. Given the competing forces of the film and substrate the permanent set will depend on the relative volume of each component. An example picture of a specimen that underwent a strain cycle and shows features of out of plane buckling is given in **Figure 1(b)**.

#### 3.3. Substrate dependence

To determine if the elastomer stiffness influences the extracted polymer thin film behavior, we prepared FLOTE specimens with PDMS of varying cross-link densities. The PDMS cross-linking agent was added to the base at a ratio of 5:1 to 15:1, with characteristic stress-strain curves given in **Figure 3(a)**. We find that the stress-strain behavior of the composite varies significantly given the difference in PDMS stiffness. However, when we extract the stress-strain behavior of the P3HT from the composite characteristics the results are quite similar, as shown in

**Figure 3(b)**. The similar response can clearly be seen in the measured Young's modulus of P3HT plotted in **Figure 3(c)**. We find that over this range in substrate stiffness, there is no clear difference in Young's modulus, yield behavior, or unloading behavior of the P3HT films.

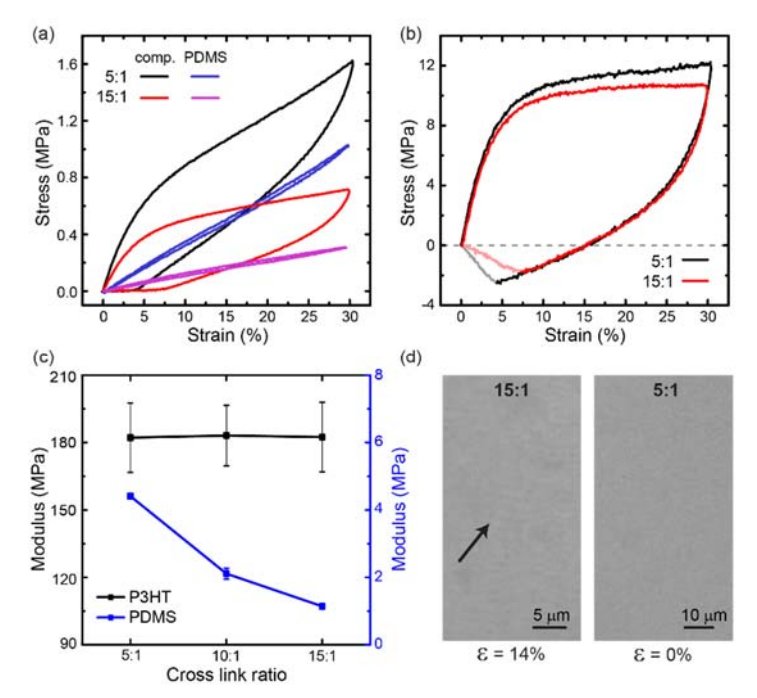


**Figure 3.** (a) Stress-strain curve of P3HT/PDMS composite and neat PDMS specimens with 15:1 and 5:1 PDMS base to cross linker ratio. The thickness of P3HT film was 100 nm. (b) Stress-strain curve of P3HT film extracted from the FLOTE tests using the composite model. (c) The elastic modulus of P3HT extracted from the composite specimen and directly measured PDMS with variation in PDMS cross-link ratio. (d) Optical microscope images of the P3HT/PDMS upon strain release to determine the point of wrinkling. In the 15:1 PDMS case wrinkles are first observed at 14% strain indicated by the black arrow, no wrinkling is observed in the 5:1 composite sample.

Previously, we observed that in a polymer film/elastomer composite that undergoes a large strain cycle the onset of wrinkling during strain removal was dependent on the substrate stiffness.<sup>24</sup> Here, we also consider when wrinkling occurs in the specimen upon removal of the applied strain. To conduct this test, we loaded the composite sample in a custom strain stage and performed a similar cyclic strain measurement as conducted in the DMA but under an optical microscope.<sup>24,31</sup> We found that for the P3HT films on 15:1 PDMS, the onset of wrinkling is observed at approximately 14% nominal strain, with microscope image given in Figure 3(d). The wrinkling amplitude then increased with further strain removal as shown in Figure S4. Comparing this to the stress-strain characteristics of the sample, the wrinkle onset strain occurs shortly after the point the P3HT film is placed in compression, consistent with inducing a wrinkling instability. In contrast, we were unable to observe wrinkling upon complete strain removal for the composite with a 5:1 PDMS substrate, as shown in Figure 3(c) and Figure S4. To further investigate wrinkling behavior upon strain removal we measured the surface profiles with a laser profilometer, with results given in Figure S5. The 15:1 sample strained to 30% and released back to 6% shows wrinkling and buckling, consistent with the onset of sample buckling when reducing the strain just past the no-load strain on the composite (i.e. permanent set). The 5:1 PDMS composite specimen held at 2% shows out of plane buckling associated with being beyond reduced past the no-load strain, but no wrinkling was observed. This may be due to the wrinkles not being discernable in the measurement methods, the critical stress for winkling onset not being met, or film yielding rather than wrinkling.<sup>24</sup> The stiffer 5:1 PDMS will reduce the wrinkling amplitude and wavelength.<sup>18</sup> The stiffer PDMS will also increase the critical stress needed to induce a wrinkling instability. 18 Some combination of these factors likely contributes to the inability to observe wrinkling in the specimen. Note that once there is out of plane wrinkling the parallel composite model is no longer accurate. Furthermore, when the composite reaches the no load point the stress in the extracted P3HT film is plotted in a lighter color in **Figure 3(b)** to highlight that this does not accurately reflect the stress in the P3HT but rather corresponds to the no-load condition on the composite. While the model may not accurately capture film stress once there is wrinkling, buckling or delamination, we plot the compressive stress on the neat films to the permanent set of the composite throughout this paper as a qualitative view of the difference in specimen behavior. For example, we find that upon strain removal the film is under relatively low compressive stress, significantly below the tensile yield stress. An additional aspect of the microscope images worth pointing out is that no delamination was observed and thus does not appear to play a role in the measured stress-strain characteristics.

#### 3.4. Film thickness dependence

The thickness limits with which the FLOTE method can accurately measure stress-strain behavior is explored by considering P3HT films with thickness from 150 nm to 20 nm, with results given in **Figure 4**. We find that the Young's modulus of the P3HT drops slightly as the film thickness decreases to 20 nm. However, this decrease is not significantly outside the variance of the Young's modulus of the other film thicknesses considered. While thin polymer film behavior can vary due to confinement effects which may be playing a role here, <sup>13</sup> there is no conclusive change in modulus for 20 nm thick films. This is consistent with other reports showing no confinement effects in 20 nm thick P3HT films, attributed to P3HT's relatively short end-to-end distance. <sup>13,25,32</sup> Considering the rest of the stress-strain response of the P3HT films we find that there does appear to be a difference in strain hardening (slope of stress-stress curve) with film thickness. We find that as the film gets thinner the strain hardening of the P3HT decreases. Upon strain removal, the unloading modulus is similar until the stress nears the no-load condition where the slope of the stress-strain curves begins to follow a similar trend as

found under tensile strain, namely that there is a reduction in the stress-strain slope for the thinner films.

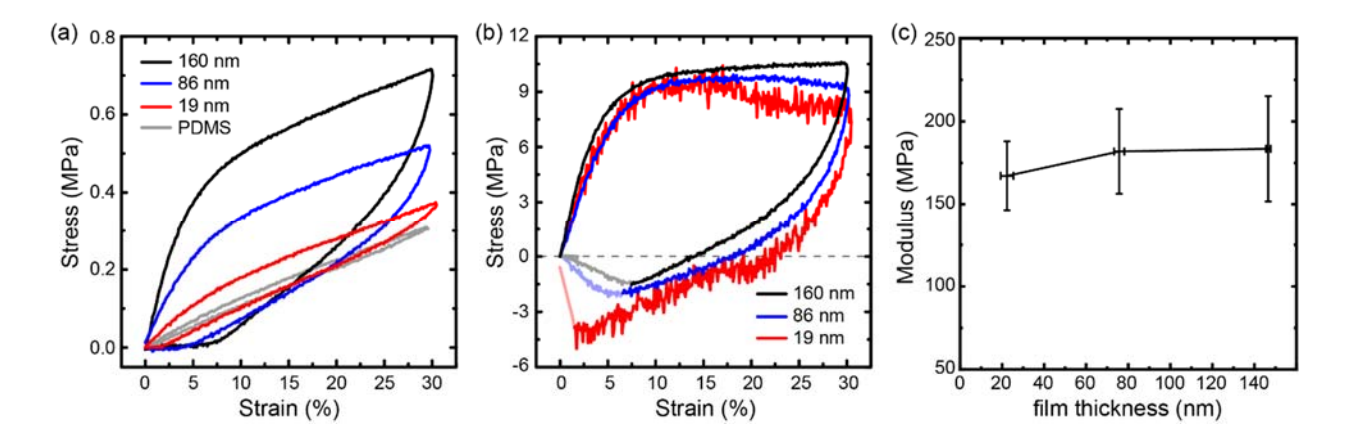


**Figure 4.** (a) Stress-strain behavior of the P3HT/PDMS composites with variation in P3HT film thickness of 150 nm, 86 nm and 19 nm. (b) stress-strain curve of the P3HT films extracted from the composite stress-strain curve. (c) The thickness dependent elastic modulus of P3HT. The PDMS stress-strain curves in (a) is a representative measurements and PDMS behavior for each film thickness considered is given in **Figure S6**.

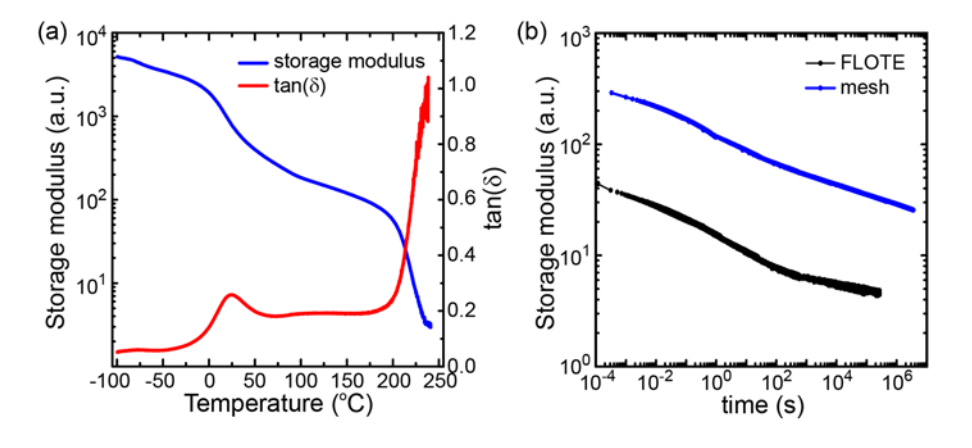


**Figure 5.** (a) Dynamic mechanical analysis temperature sweep of drop cast P3HT on a glass fiber mesh. (b) Stress relaxation behavior of P3HT/PDMS composite specimen (P3HT thickness

of 130 nm) and P3HT measured using the glass fiber mesh. The absolute modulus cannot be determined using the glass mesh approach and the stress relaxation plots are offset for clarity. The master curve is created from individual relaxation tests given in **Figure S7**. The reference temperature was 20°C.

#### 3.5. Temperature and strain rate dependence

A major advantage of this approach over other thin film test methods is the ability to test the films in a temperature controlled chamber. This allows for the films to be tested over a broad temperature range to probe viscoelastic behavior. Here we consider the temperature dependent behavior of the P3HT films, with particular interest in temperatures above and below the polymer's glass transition temperature (Tg). To determine the Tg of the P3HT, dynamic mechanical tests were performed by drop casting the P3HT onto a glass fiber mesh using an approach previously reported.<sup>33</sup> The specimen was then loaded into the DMA and scanned over a broad temperature range while under an oscillating 0.01% tensile strain 1 Hz frequency. The results are given in Figure 5(a), showing a clear  $T_g$  at 25°C as defined by the peak in  $tan(\delta)$ . Thus, we performed tensile tests of the FLOTE specimens at -10°C, 30°C, and 50°C. The results of the composite specimen and neat PDMS are plotted in Figure 6(a), while the extracted P3HT film behavior is given in Figure 6(b). We found that the Young's modulus of PDMS is approximately 1.2 MPa independent of the temperature. This is expected given that PDMS will be in the rubbery plateau over this temperature range. Meanwhile, the behavior of P3HT changed significantly as the specimen temperature increased from -10°C to 30°C, where we find that the Young's modulus decreases from 1.6 GPa to 200 MPa as given in Figure 6(c). In addition to Young's modulus, features of the stress strain curve including the yield strength, yield strain, and strain hardening behavior show a clear temperature dependence as well. When the specimen is at -10°C there is a clear yield point at a relatively low strain of 4.3% and high yield stress of 44.4 MPa. Heating the specimen to 50°C results in a significantly larger yield strain (~8%) and low yield stress (~4 MPa). The FLOTE tests also provide insight into features of the P3HT response upon unloading. As the applied strain is removed, there is a clear difference in the unloading modulus of the P3HT depending on sample temperature. This leads to the no-load strain of the film upon strain removal to decrease significantly when tested above the Tg of P3HT.

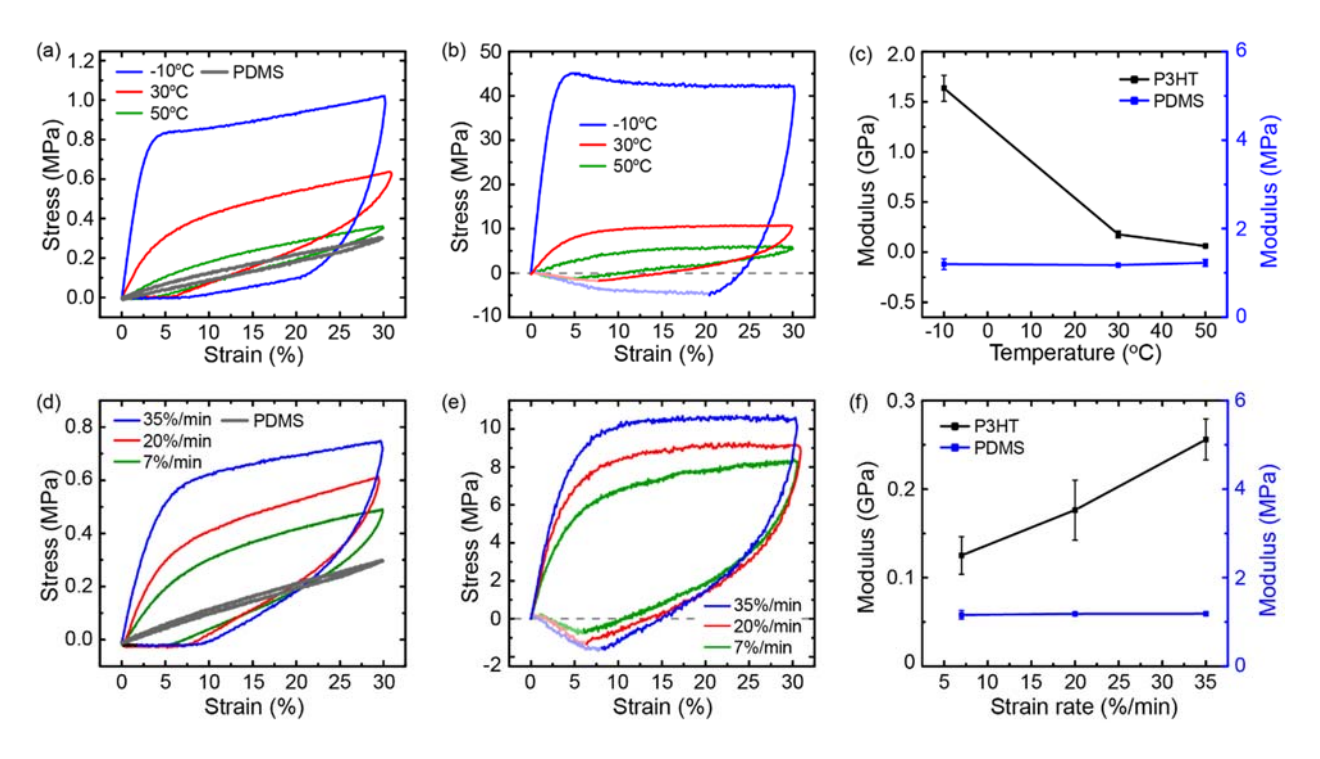


**Figure 6.** (a) Stress-strain curves of P3HT/PDMS composite specimens tested at -10°C, 30°C, and 50°C, all specimens were tested with strain rate 20%/min, P3HT film thickness were approximately 100 nm. (b) Stress-strain behavior of P3HT film extracted from the FLOTE tests. c) Temperature dependent Young's modulus of P3HT and PDMS. d) Stress-strain curves of P3HT/ PDMS composite samples with a strain rate of 35%/min, 20%/min, and 7%/min, all tested at 30°C. (e) Stress-strain behavior of P3HT extracted from data in (d). Strain rate dependent Young's modulus of P3HT and PDMS. The PDMS stress-strain curves in (a) and (d)

are representative measurements and corresponding data for each test condition is provided in Figure S8.

The FLOTE method is also able to accurately capture the strain rate dependence of P3HT. We consider three different strain rates of 35%/min, 20%/min, and 7%/min at a temperature of 30°C. The stress-strain response under these different strain rates is given in **Figure 6(d,e)**, and the extracted Young's moduli of the P3HT and PDMS are given in **Figure 6(f)**. Similar to the temperature dependence, the PDMS behavior is relatively constant over this range of strain rate. On the other hand, the P3HT films show a clear strain rate dependence with Young's modulus increasing from 125 MPa to 266 MPa. The Young's moduli are comparable to values reported in the literature, which vary from 135 MPa to 360 MPa over a strain range of 1.2 %/min to 60 %/min.<sup>25</sup>

#### 3.6. Stress relaxation modulus

Another important feature associated with polymer viscoelasticity is stress relaxation. A common approach to capture stress relaxation behavior of a polymer is to hold the specimen under a small tensile strain for a prescribed period of time and monitor the load on the sample. The test is then repeated over a range of temperatures, with a designated recovery time between tests. A master curve is generated from the various measurements using the time-temperature superposition principle to capture the viscoelastic behavior of the polymer over a broad time scale.<sup>34</sup> Similar to tensile tests, this measurement is typically done on bulk samples. However, a number of alternative approaches have been developed to conserve material. For example, one can use the glass mesh approach as discussed above to measure the Tg of P3HT. However, the drop cast nature of the film may not accurately represent the thin film morphology used in

devices. Alternatively, FOE wrinkling dynamics have also been demonstrated to capture stress relaxation.<sup>20</sup> However, this method typically requires optical access to the specimen for laser diffraction measurements as well as temperature control, which can be a challenge. Here, we show that stress relaxation can also be accurately measured using the FLOTE approach.

The stress relaxation of P3HT was measured by placing the FLOTE specimen in 2% tensile strain and holding for 10 minutes followed by 15 minutes recovery. This was done over a temperature range of -10°C to 60°C in increments of 10°C. From these measurements a master curve was created by fitting to the Williams Landel Ferry (WLF) function, with results given in Figure 5(b). The relaxation behavior of a neat PDMS sample under similar test conditions is given in Figure S7(c) showing that the stress is significantly lower than the composite specimen and thus the stress relaxation of the composite reflects the P3HT behavior. To assess the accuracy of the method, it is compared to stress relaxation measured using the glass mesh specimens discussed above. We find that the two approaches result in similar stress relaxation profiles demonstrating the ability of the FLOTE method to effectively measure thin film relaxation. There are minor differences in relaxation behavior between approaches, which is largely the result of the drop in the modulus over a loading time associated with the glass transition of P3HT. This is attributed to differences in P3HT morphology, where the drop cast specimens likely have greater crystallinity than the spun cast films resulting in a diminished change in relaxation behavior across the glass transition. This highlights the importance of using device relevant films for stress relaxation measurements and the strengths of the FLOTE method.

#### 3.7. Cyclic loading

Multiple loading events are expected in stretchable devices and thus it is important to consider the stress-strain behavior of the film under cyclic loading. The stress-strain curves of the composite specimen held at 30°C over 50 strain cycles are given in Figure 7(a). As demonstrated for one strain cycle above, clear hysteresis in the stress-strain curve is observed attributed to energy dissipation in the P3HT due to viscoelastic - plastic deformation. During unloading of the specimen in the first strain cycle, the P3HT film is placed in compression and film wrinkling is expected followed by specimen buckling. In Figure 7(a), the composite specimen's no-load state upon strain removal is found at ~5% strain where buckling is expected to occur. Upon the second loading, the stress in the specimen begins to increase at approximately 2.5% strain. The difference between no-load strain upon unloading and the increase in stress during the second cycle suggests viscoelastic recovery of the P3HT. The stress in the second tensile strain is found to be significantly lower than the first cycle at low strains and approaches the initial stress at 30% strain. This behavior is similar to that found in some elastomers and elastomer composites, referred to as strain softening. This behavior is a feature of the Mullins' effect discussed further below. Additional strain cycles have similar stress-strain behavior as the second loading cycle with a slowly decreasing stress in both tension and compression and a narrowing of the hysteresis behavior. We also consider cyclic loading of a P3HT/PDMS specimen held at 50°C. As shown in Figure 7(b), the film is more compliant as expected. Under cyclic strain, there is a drop in the stress in the film upon the second applied tensile strain similar to the sample held at 30°C, but to a significantly lower extent. We also find lower hysteresis with cyclic strain, and less stress-strain changes with the number of strain cycles. The stability in the stress-strain curve after several strain cycles implies stabilized viscoelastic hysteresis behavior.<sup>35</sup>

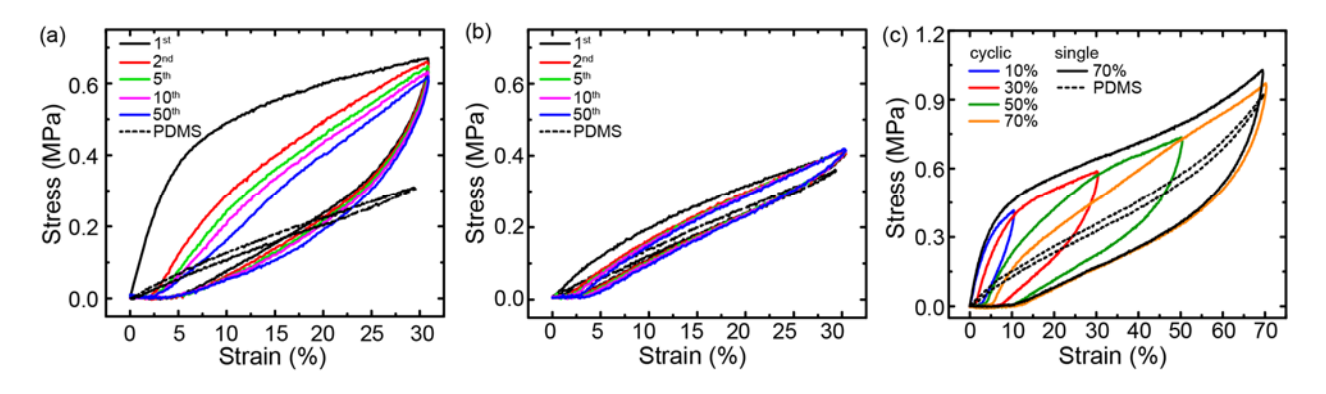


**Figure 7**. Stress-strain curve of P3HT/PDMS composite specimens with 30% cyclic strain (a) strained for 50 cycles at 30°C, and (b) strained for 50 cycles at 50°C. (c) P3HT/PDMS composite with cyclic variable strain range of 10% to 70% strain in increments of 20% along with a virgin composite sample and neat PDMS strained directly to 70% (single). The specimen temperature was 30°C. P3HT film thickness in each case is approximately 80 nm.

#### 3.8. Strain range

The results thus far have focused on a strain range of 30%, but larger strains are easily accessible with this method. **Figure 7(c)** shows a variation in strain range, cyclically stretching a film with increasing strain ranges from 10% to 70% strain. A virgin composite sample and a neat PDMS sample are also strained directly to 70% with results given in **Figure 7(c)**. Again, the features of the cyclic tests with increasing strain magnitude are consistent with the Mullins' effect. <sup>35-37</sup> These features include strain softening after the first loading cycle, clear hysteresis in the stress-strain curves upon unloading and reloading, and during cyclic loading when the strain exceeds the previous maximum strain the stress-strain curve closely follows the virgin specimen. Another feature associated with the Mullins' effect is an increase in permanent set when the sample is strained to greater extents. <sup>38</sup> We also observe this behavior in the composite samples where the permanent set is found to increase as it undergoes larger tensile strains. The Mullins'

effect is most commonly observed in elastomer composites, and the polymer film on the elastomer substrate considered here is similar in that regard.

#### 4.0. Discussion

The FLOTE method has similarities with other film test methods and the mechanical behavior of the P3HT can be compared to previous reports. We find that the elastic modulus and yield stress is similar to other reports. 17,25 The variation in elastic modulus with strain rate, and the unloading stress-strain behavior is similar to that reported by Zhang et al. using FOW tests.<sup>25</sup> However, the FLOTE methods also has a number of important advancements. These differences include testing on an elastomer support, which increases the P3HT fracture strain relative to freestanding and films floated on water. Thus the strain limits that may be applied in devices can be probed. Upon removal of a tensile load the composite also places the P3HT in compression, which is not possible with free-standing or FOW tests. In addition, it is critically important that the films can be tested over a broad temperature range, something that is inaccessible with FOW tests. While the FOW tests can vary strain rate and probe stress relaxation. The ability to test samples over a broad temperature range allows for a larger thermomechanical property space to be investigated. This is a central advantage of the FLOTE method and leads to the ability to capture detailed thermomechanical characteristics of the composite that have direct implications for intrinsically stretchable devices. The two features of the stress-strain behavior that are specifically focused on in this discussion are the stress response of the film when removing a large applied tensile strain and the hysteresis behavior of the composite under cyclic loading. Importantly for context, many of the most successful intrinsically stretchable devices are based on composites that embed polymer semiconductor nano-fibrils within an elastomer matrix.<sup>7,8</sup> While a simple parallel composite is studied here, we believe that many of the insights from

these samples are applicable to other polymer semiconductor/elastomer composite configurations. This is supported by the similarity of the stress-strain characteristics of the FLOTE specimens to other thermoplastic elastomers and elastomer composites.<sup>35,39</sup>

To start, consider the removal of an applied strain on the composite and the point at which the film is placed in compression. For the specimen that was held below P3HT's glass transition temperature (-10°C), under a tensile strain there is a clear yield stress followed by cold drawing. When the strain is removed, the P3HT film is placed in compression after little strain removal (24% nominal strain). Continued strain removal results in specimen buckling. For a thick elastomer substrate that reduces the permanent set and constrains buckling this likely results in film wrinkling then folding and possibly delamination.<sup>24</sup> This would be highly undesirable for stable stretchable device operation. For the sample held at 50°C, the strain at which the film is placed into compression upon unloading is significantly lowered (15.5% strain). Being above P3HT's T<sub>g</sub> results in greater compliance and faster stress relaxation, both of which contribute to the drop in the no-load strain. The state of P3HT at higher temperatures also results in lower compressive stress upon further strain removal. In addition to the viscoelastic character of the film, it is observed that the stiffer PDMS also impacts the wrinkling characteristics of the film under compression. These results suggest that managing the viscoelastic characteristics of the conjugated polymer and the modulus mismatch between the polymer and elastomer may be an effective approach to minimize the stress in the film under cyclic strain and limit wrinkling and thus improve the stability of the film in stretchable applications.

Turning to hysteresis of the composite, first consider one strain cycle as given in **Figure 6**. Over this strain cycle the hysteresis is clearly largest for the specimen at -10°C and decreases considerably as the sample temperature is increased. The large hysteresis behavior of the low

temperature sample is associated with energy dissipation through plastic flow. Increasing the sample temperature decreases the hysteresis characteristics as the film becomes more compliant and viscoelastic. Considering the 30°C sample, plastic deformation is still expected in the initial applied strain where a relatively clear yield point is observed at 5% strain. The plastic flow of the polymer upon large applied strain likely contributes to the strain softening observed upon the second strain cycle. This is supported by previous observations of aggregate order decreasing in conjugated polymer films under large applied strains.<sup>26,40</sup> The inelastic deformation also results in a permanent set of the composite after strain removal. The hysteresis behavior after the first strain cycle remains similar but with a continuous drop in the stress throughout the strain cycle. The hysteresis behavior can be broken down into a stable and unstable component. The stable hysteresis character is associated with energy dissipation related to the viscoelastic characteristics of the polymer. The unstable component is associated with an irreversible process that may include morphological degradation or delamination of the film. In a previous report by Tianlei et. al, delamination of P3HT from PDMS was observed for films subject to large cyclic strains that became more severe with the number of strain cycles.<sup>41</sup> Thus, we suspect that delamination may be contributing to the unstable hysteresis character. When the film is more compliant (by increasing the sample temperature), the hysteresis behavior of the composite is much smaller (Figure 7(b)). In this case, less delamination is expected under cyclic loading improving stable deformation characteristics. The stable hysteresis is believed to be from limiting plastic flow of the P3HT. Thus, targeting polymers that have viscoelastic characteristics similar to P3HT significantly above its T<sub>g</sub> may improve stable operation. These results may help explain the success of employing polymer semiconductor nano-fibrils in an elastomer matrix where nano-confinement is proposed as a mechanism to improve stretchability. By using confinement to modify viscoelastic characteristics, the conjugated polymer may avoid being placed under large compressive stress during a given strain cycle.

Comparing the results to other elastomer composites is also potentially very instructive, particularly the similarities with the Mullins' effect. The Mullins' effect and hysteresis in elastomers have been widely studied and there are a number of constitutive models that reproduce this unique stress-strain behavior. For example, thermoplastic polyurethane elastomer that shows clear Mullins' effect was constitutively modeled as hyperelastic, viscoelastic-plastic by Qi and Boyce.<sup>35</sup> This model consisted of a hyperelastic spring in parallel with the viscoelastic-plastic element, which in our case would be the PDMS and P3HT respectively. The similarities to this model suggest similar constitutive models may be applicable to polymer semiconductor elastomer composites providing a framework to understand mechanical behavior under various loading conditions and to design composite systems with stable behavior in stretchable applications.

#### 5.0. Conclusion

A novel approach to measure the thermomechanical properties of conjugated polymers with a focus on P3HT was presented. We show that by using a thin PDMS elastomer support for a polymer semiconductor thin film, the specimen handling becomes manageable and the sample can be tested in a high performance DMA system. We show that these tests are able to accurately obtain the stress-strain behavior of the P3HT over large applied strains in multiple loading cycles, and over a large range in strain rates and sample temperatures. Probing the film while on an elastomer support also captures the impact of the neighboring elastomer on the film's mechanical behavior. Results from the measurements show that there is no change in Young's modulus of P3HT with film thickness down to 20 nm, however there does appear to be some

changes in strain hardening behavior with film thickness. The measurements under cyclic strain also showed that the hysteresis behavior of the composite had features consistent with the Mullins' effect and that hysteresis was highly dependent on the specimen temperature. In addition to the stress-strain curves of the polymer, we show that the FLOTE method is also able to capture stress relaxation of device relevant thin films over broad time scales. Through these measurements a number of insights into the behavior of conjugated polymer–elastomer composites are made that have important implications for stretchable devices. This includes capturing key viscoelastic-plastic characteristics of the polymer thin films that directly impact the stability of the composite under cyclic strain. The temperature dependent mechanical response of P3HT suggests that designing other polymer semiconductor systems with appropriate viscoelastic behavior can lead to stable stretchable device operation. Thus, the FLOTE approach is a powerful tool to assist in assessing the potential for conjugated polymers to be successful in stretchable applications.

#### ASSOCIATED CONTENT

**Supporting Information**. FEA stress-strain results, film on water tensile tests data, optical microscope of FLOTE specimens at various applied strains, individual stress-strain curves for FLOTE specimens with corresponding neat PDMS substrate, and WLF fit to stress relaxation measurements.

#### **AUTHOR INFORMATION**

#### **Corresponding Author**

\* btoconno@ncsu.edu

### ACKNOWLEDGMENT

This work was supported by the National Science Foundation Award No. 1728370 and Award No. 1554322.

#### REFERENCES

- (1) Park, J. S.; Chae, H.; Chung, H. K.; Lee, S. I. Thin Film Encapsulation for Flexible AM-OLED: A Review. *Semicond. Sci. Technol.* **2011**, *26*, 3.
- (2) Boutry, C. M.; Negre, M.; Jorda, M.; Vardoulis, O.; Chortos, A.; Khatib, O.; Bao, Z. A Hierarchically Patterned, Bioinspired e-Skin Able to Detect the Direction of Applied Pressure for Robotics. *Sci. Robot.* **2018**, *6914*, 1–10.
- (3) Kim, J.; Lee, M.; Shim, H. J.; Ghaffari, R.; Cho, H. R.; Son, D.; Jung, Y. H.; Soh, M.; Choi, C.; Jung, S.; Chu, K.; Jeon, D.; Lee, S.; Kim, J.; Choi, S.; Hyeon, T.; Kim, D. Stretchable Silicon Nanoribbon Electronics for Skin Prosthesis. *Nat. Commun.* **2014**, *5*, 1–11.
- (4) Kaltenbrunner, M.; White, M. S.; Głowacki, E. D.; Sekitani, T.; Someya, T.; Sariciftci, N. S.; Bauer, S. Ultrathin and Lightweight Organic Solar Cells with High Flexibility. *Nat. Commun.* **2012**, *3*.
- (5) Kim, T.; Kim, J.; Kang, T. E.; Lee, C.; Kang, H.; Shin, M.; Wang, C.; Ma, B.; Jeong, U.; Kim, T.; Kim, B. J. Flexible, Highly Efficient All-Polymer Solar Cells. *Nat. Commun.* **2015**, *6*, 1–7.
- (6) Kim, J.; Kim, J.; Lee, W.; Yu, H.; Kim, H. J.; Song, I.; Shin, M.; Oh, J. H.; Jeong, U.; Kim, T.; Kim, B. J. Tuning Mechanical and Optoelectrical Properties of Poly(3-Hexylthiophene) through Systematic Regionegularity Control. *Macromolecules* **2015**, *48*, 4339–4346.
- (7) Xu, J.; Wang, S.; Wang, G. N.; Zhu, C.; Luo, S.; Jin, L.; Gu, X.; Chen, S.; Feig, V. R.; To, J. W. F.; Rondeau-Gagné, S.; Park, J.; Schroeder, B. C.; Lu, C.; Oh, J.; Wang, Y.; Kim, Y.; Yan, H.; Sinclair, R.; Zhou, D.; Xue, G.; Murmann, B.; Linder, C.; Cai, W.; Tok, J. B. H.; Chung, J.;

- Bao, Z. Highly Stretchable Polymer Semiconductor Films through the Nanoconfinement Effect. *Science*, **2017**, *64*, 59–64.
- (8) Zhang, G.; McBride, M.; Persson, N.; Lee, S.; Dunn, T. J.; Toney, M. F.; Yuan, Z.; Kwon, Y. H.; Chu, P. H.; Risteen, B.; Reichmanis, E. Versatile Interpenetrating Polymer Network Approach to Robust Stretchable Electronic Devices. *Chem. Mater.* **2017**, *29*, 7645–7652.
- (9) Mun, J.; Wang, G. J. N.; Oh, J. Y.; Katsumata, T.; Lee, F. L.; Kang, J.; Wu, H. C.; Lissel, F.; Rondeau-Gagné, S.; Tok, J. B. H.; Bao, Z. Effect of Nonconjugated Spacers on Mechanical Properties of Semiconducting Polymers for Stretchable Transistors. *Adv. Funct. Mater.* **2018**, *28*, 1–10.
- (10) Wang, S.; Xu, J.; Wang, W.; Wang, G. J. N.; Rastak, R.; Molina-Lopez, F.; Chung, J. W.; Niu, S.; Feig, V. R.; Lopez, J.; Lei, T.; Kwon, S.; Kim, Y.; Foudeh, A. M.; Ehrlich, A.; Gasperini, A.; Yun, Y.; Murmann, B.; Tok, J. B. H.; Bao, Z. Skin Electronics from Scalable Fabrication of an Intrinsically Stretchable Transistor Array. *Nature* **2018**, *555*, 83–88.
- (11) Yu, Z.; Niu, X.; Liu, Z.; Pei, Q. Intrinsically Stretchable Polymer Light-Emitting Devices Using Carbon Nanotube-Polymer Composite Electrodes. *Adv. Mater.* **2011**, *23*, 3989–3994.
- (12) O'Connor, B. T.; Awartani, O. M.; Balar, N. Morphological Considerations of Organic Electronic Films for Flexible and Stretchable Devices. *MRS Bull.* **2017**, *42*, 108–114.
- (13) Forrest, J. A.; Dalnoki-Veress, K.; Dutcher, J. R. Interface and Chain Confinement Effects on the Glass Transition Temperature of Thin Polymer Films. *Phys. Rev. E.* **1997**, *56*, 5705–5716.

- (14) Forrest, J. A.; Dalnoki-Veress, K.; Stevens, J. R.; Dutcher, J. R. Effect of Free Surfaces on the Glass Transition Temperature of Thin Polymer Films. *Phys. Rev. Lett.* **1996**, *77*, 2002–2005.
- (15) Stafford, C. M.; Harrison, C.; Beers, K. L.; Karim, A.; Amis, E. J.; Vanlandingham, M. R.; Kim, H.; Volksen, W.; Miller, R. D.; Simonyi, E. V. A. E. A Buckling-Based Metrology for Measuring the Elastic Moduli of Polymeric Thin Films. *Nat. Mater.* **2004**, *3*, 545–550.
- (16) Kim, J.; Nizami, A.; Hwangbo, Y.; Jang, B.; Lee, H.; Woo, C.; Hyun, S.; Kim, T. Tensile Testing of Ultra-Thin Films on Water Surface. *Nat. Commun.* **2013**, *4*, 1–6.
- (17) Root, S. E.; Savagatrup, S.; Printz, A. D.; Rodriquez, D.; Lipomi, D. J. Mechanical Properties of Organic Semiconductors for Stretchable, Highly Flexible, and Mechanically Robust Electronics. *Chem. Rev.* **2017**, *117*, 6467–6499
- (18) Chung, J. Y.; Nolte, A. J.; Stafford, C. M. Surface Wrinkling: A Versatile Platform for Measuring Thin-Film Properties. Adv. *Mater.* **2011**, *23*, 349–368.
- (19) Stafford, C. M.; Vogt, B. D.; Harrison, C.; April, R. V; Re, V.; Recei, M.; June, V. Elastic Moduli of Ultrathin Amorphous Polymer Films. *Macromolecules* **2006**, *39*, 5095–5099.
- (20) Chung, J. Y.; Douglas, J. F.; Stafford, C. M.; Chung, J. Y.; Douglas, J. F.; Stafford, C. M. A Wrinkling-Based Method for Investigating Glassy Polymer Film Relaxation as a Function of Film Thickness and Temperature. *J. Chem. Phys.* **2017**, *154902*.
- (21) Kim, H. J.; Kim, J.; Ryu, J.; Kim, Y.; Kang, H.; Lee, W. B.; Kim, T.; Kim, B. J.; Al, K. I. M. E. T. Architectural Engineering of Rod À Coil Compatibilizers for Producing Mechanically and Thermally Stable Polymer Solar Cells. *ACS Appl. Mater. Interfaces* **2014**, *10*, 10461–10470.

- (22) Liu, Y.; Chen, Y. C.; Hutchens, S.; Lawrence, J.; Emrick, T.; Crosby, A. J. Directly Measuring the Complete Stress-Strain Response of Ultrathin Polymer Films. *Macromolecules* **2015**, *48*, 6534–6540.
- (23) Bay, R. K.; Crosby, A. J. Uniaxial Extension of Ultrathin Freestanding Polymer Films. *ACS Macro Lett.* **2019**, 1080–1085.
- (24) Sun, T.; Song, R.; Balar, N.; Sen, P.; Kline, R. J.; O'Connor, B. T. Impact of Substrate Characteristics on Stretchable Polymer Semiconductor Behavior. *ACS Appl. Mater. Interfaces* **2019**, *11*, 3280–3289.
- (25) Zhang, S.; Ocheje, M. U.; Luo, S.; Ehlenberg, D.; Appleby, B.; Weller, D.; Zhou, D.; Rondeau-Gagné, S.; Gu, X. Probing the Viscoelastic Property of Pseudo Free-Standing Conjugated Polymeric Thin Films. *Macromol. Rapid Commun.* **2018**, *1800092*, 1–8.
- (26) Scott, J. I.; Xue, X.; Wang, M.; Kline, R. J.; Hoffman, B. C.; Dougherty, D.; Zhou, C.; Bazan, G.; O'Connor, B. T. Significantly Increasing the Ductility of High Performance Polymer Semiconductors through Polymer Blending. *ACS Appl. Mater. Interfaces* **2016**, *8*, 14037–14045.
- (27) Rodriquez, D.; Kim, J.; Root, S.E.; Fei, Z.; Boufflet, P.; Heeney, M.; Kim, T.; Lipomi, D.J.; Comparison of Methods for Determining the Mechanical Properties of Semiconducting Polymer Films for Stretchable Electronics. ACS Appl. Mater. Interfaces **2017**, *9*, 8855–8862.

- (28) Crowe-Willoughby, J. A.; Weiger, K. L.; Ozcam, A. E.; Genzer, J. Formation of Silicone Elastomer Networks Films with Gradients in Modulus. *Polymer.* **2010**, *51*, 763–773.
- (29) Chambon, F.; Winter, H. H. Linear Viscoelasticity at the Gel Point of a Crosslinking PDMS with Imbalanced Stoichiometry. *J. Rheol.* **1987**, *31*, 683–697.
- (30) Li, T.; Huang, Z.; Suo, Z.; Lacour, S. P.; Wagner, S. Stretchability of Thin Metal Films on Elastomer Substrates. *Appl. Phys. Lett.* **2004**, *85*, 3435–3437.
- (31) Awartani, O. M.; Zhao, B.; Currie, T.; Kline, R. J.; Zikry, M. A.; O'Connor, B. T. Anisotropic Elastic Modulus of Oriented Regioregular Poly(3-Hexylthiophene) Films. *Macromolecules* **2016**, *49*, 327–333.
- (32) McCulloch, B.; Ho, V.; Hoarfrost, M.; Stanley, C.; Do, C.; Heller, W. T.; Segalman, R. A. Polymer Chain Shape of Poly(3-Alkylthiophenes) in Solution Using Small-Angle Neutron Scattering. *Macromolecules* **2013**, *46*, 1899–1907.
- (33) Andersson, B.; Sjögren, A.; Berglund, L. Micro- and Meso-Level Residual Stresses in Glass-Fiber/Vinyl-Ester Composites. *Compos. Sci. Technol.* **2000**, *60*, 2011–2028.
- (34) Fox, A. Eds. *Stress Relaxation Testing*. ASTM International: West Conshohocken, PA, 1979.
- (35) Qi, H. J.; Boyce, M. C. Stress-Strain Behavior of Thermoplastic Polyurethanes. *Mech. Mater.* **2005**, *37*, 817–839.
- (36) Diani, J.; Fayolle, B.; Gilormini, P. A Review on the Mullins Effect. *Eur. Polym. J.* **2009**, 45, 601–612.

- (37) Drozdov, A. D. Mullins' Effect in Semicrystalline Polymers. *Int. J. Solids Struct.* **2009**, *46*, 3336–3345.
- (38) Dorfmann, A.; Ogden, R. W. A Constitutive Model for the Mullins Effect with Permanent Set in Particle-Reinforced Rubber. *Int. J. Solids Struct.* **2004**, *41*, 1855–1878.
- (39) Diani, J.; Fayolle, B.; Gilormini, P. A Review on the Mullins Effect. *European Polymer Journal*. 2009.
- (40) Zhang, S.; Ocheje, M. U.; Huang, L.; Galuska, L.; Cao, Z.; Luo, S.; Cheng, Y. H.; Ehlenberg, D.; Goodman, R. B.; Zhou, D.; Liu, Y.; Chiu, Y.; Azoulay, J. D.; Rondeau-Gagné, S.; Gu, X.. The Critical Role of Electron-Donating Thiophene Groups on the Mechanical and Thermal Properties of Donor–Acceptor Semiconducting Polymers. *Adv. Electron. Mater.* **2019**, *5*, 1–11.
- (41) Sun, T.; Scott, J. I.; Wang, M.; Kline, R. J.; Bazan, G. C.; O'Connor, B. T. Plastic Deformation of Polymer Blends as a Means to Achieve Stretchable Organic Transistors. *Adv. Electron. Mater.* **2017**, *3*, 1–10.

## **Table of content graphic**

